Al-khwarizmi Engineering Journal

Al-Khwarizmi Engineering Journal, Vol.2, No.1,pp 15-34, (2006)

A Study Of Strengthening Circular Diaphragm By Ring-Shaped Concentric Ribs

Dr. Somer M. Nacy
University of Baghdad

Dr.Hikmat Al-Rawi
University of Al-Anbar

Mohammed M. Hasan
University of Al-Anbar

(Received 21 September 2005; accepted 4 May 2006)

Abstract:-

This paper deals with the determination of stresses and deflections of clamped circular diaphragm strengthened by one or two ring-shaped concentric ribs, under uniform static and dynamic pressures. The simulation has been achieved by using the well-known engineering software finite element package *MSC/NASTRAN*.

As a design study, the effect of using a clamped ring, and the effect of using a ring-shaped rib on both surfaces of diaphragm instead of one, has been discussed in this work. To show the effectiveness of this study, results of this work have been compared with published data [1].

In the conclusion, the authors underline the validity of the considered design study, and the optimization of strengthened diaphragms.

Keywords **:** diaphragm, Nastran, Static, Dynamic.

1.Introduction

The diaphragm is the subsystem that distributes lateral load to the perpendicular subsystems and that provides lateral support. Diaphragms are treated as horizontal beams. The upper (or lower) surface, which is analogous to the web of a wide-flange beam, is assumed to carry the shear; the edge, which is analogous to the flange, is assumed to carry the flexural stress [2].

Several researches have recently been published regarding the stress and deflection characteristics of diaphragms for application to pressure sensors [3,4], microvalves [5], microphones [6] and other acoustic devices. For these devices, the applied load is assumed to be constant over the diaphragm surface [7].

In this work, analytical investigation for a clamped circular diaphragm strengthened by one or two ring-shaped concentric ribs, with built-in stress and large deflections are presented. The advantages of the circular diaphragm consist of good technological, mechanical and measuring properties [1].

In general, analytical and exact variational solutions for diaphragm behavior are desirable because of their

ease of use and the insight they provide to the designer. Specific geometric effects can be ascertained from these solutions. However, these solutions are generally only applicable for small deflections. Numerical techniques, such as finite element analysis, boundary element analysis, and finite difference analysis, can be more accurate in predicting stresses and deflections, especially for large deflections. Unfortunately, these techniques generally require more effort to use and may not supply the same insight as analytical or exact variational solutions. The use of plate theory is appropriate for the analysis of diaphragms [7]; therefore, this work has been achieved by using the finite element software package *MSC/NASTRAN* with plate bending and shell elements.

As a verification test, and to show the effectiveness of this work, a model similar to one used by a published research [1] has been built in *MSC/NASTRAN* in order to make a comparison between this published research, and the present work.

2.Finite Element Analysis

Finite element procedures have become an important and frequently indispensable part of engineering analysis and design. Finite element computer programs are now widely used in practically all branches of engineering [8].

Applications range from deformation and stress analysis of automotive, aircraft, building, and bridge structures to field analysis of heat flux, fluid flow, magnetic flux, seepage, and other flow problems. With the advances in computer technology and *CAD* systems, complex problems can be modeled with relative ease. Several alternative configurations can be tried out on a computer before the first prototype is built [9].

The development of finite element methods for the solution of practical engineering problems began with the advent of the digital computer. That is, the essence of a finite element solution of an engineering problem is that a set of governing algebraic equations is established and solved, and it was only through the use of the digital computer that this process could be rendered effective and given general applicability. These two properties-effectiveness and general applicability in engineering analysis are inherent in the theory used and have been developed to a high degree for practical computations, so that finite element methods have found wide appeal in engineering practice.

3.Case Studies

Except the cases used to compare the published data, all of the models used are of the same radius (R = 50mm) and same material (pure, annealed copper) with the following properties [11] :

Modulus of elasticity, **E** = 119 GPa.

Modulus of rigidity, **G** = 44.7 GPa.

Poisson's ratio, $\boldsymbol{\nu}$ = 0.326

Yield stress, $\boldsymbol{\sigma_y}$ = 70 MPa.

Mass density, $\boldsymbol{\rho}$ = 8.96 g/cm^3.

Fig.(1) shows the schematic view of the base model used (flat diaphragm) with thickness (h = 0.1mm) and radius (R = 50mm).

The maximum allowable static pressure that the flat diaphragm can sustain without exceeding the elastic limit may be calculated as [12]:

$$\mathbf{P_y = \frac{4h^2}{3R^2}\sigma_y}$$, Sdi,eas $\mathbf{P_y = 373.3\,Pa.}$

a *safety factor* (S.F. = 1.5), the uniform pressure used is (P = 250Pa) for the static loading, and

this value has been proposed as a peak pressure for the dynamic analysis to work within elastic limit.

In order to strength the diaphragm, one or two ring-shaped concentric ribs are used. For this case, two new studies are presented in this work; they are :

1. Study the effect of using a ring-shaped rib on both of the upper and lower diaphragm surfaces instead of one surface.
2. Study the effect of using clamped ring (built-in with the clamped edges of the diaphragm).

To do so, a ring-shaped rib (of the same material as is the diaphragm) with thickness (H = 0.1mm) and radial width (br = 2mm) is used at (25) radial positions, from r = 1mm (bossed material) to r = 49mm (clamped ring) as shown in figures (2-9). The effectiveness of these studies is clearly appeared by making a comparison with the published research [1].

Fig.(10) shows the schematic view of the model, which had been used in this published research [1]; where :

R = 75mm, h = 4mm, H = 6mm, br = 4mm, r_1 = 20mm, r_2 = 60mm

and the pressure used was (**P** = 3KPa). The properties of this model were :

Modulus of elasticity, **E** = 17.87 MPa., *Poisson's ratio*, $\boldsymbol{\nu}$ = 0.48

To achieve the comparison, similar model has been built in *MSC/NASTRAN* package; and another models with the same properties but with different choices for the dimensions and positions of stiffeners, are used to prove the effectiveness of the design study that has been achieved in this work.

For the dynamic analysis, two types of transient loading are used; they are :

1. Continuous absolute sine load, at frequency (f = 40Hz).
2. Absolute sine-pulse load, at the first natural frequency of every case.

The dynamic pressure function of these two types of transient loading is :

$$\mathbf{P} = \mathbf{250}\left[\left|\sin(\boldsymbol{\pi} f t)\right|\right]$$

where (f, t) represent the frequency (Hz), and time (sec.) respectively; and the transient pressure (P) is measured in (Pa).

For all the cases used at the dynamic analysis part, damping does not be considered (zero damping).

Every model used in the finite elements package *MSC/NASTRAN* is divided into triangular and quadrilateral plate bending and shell elements. All of these elements are subjected to uniform pressure and the edges are completely fixed.

4.Static Analysis

The aim of this analysis is to investigate the stresses and deflections of clamped circular diaphragm strengthened by one or more ring-shaped ribs.

The two studies explained previously are presented here and compared with the published data.

➢ **Effect of Radial Position of The Ring** To show the effect of using ring-shaped ribs on the two surfaces of the diaphragm instead of one surface and the effective use of clamped ring, fifty models are used here at twenty five radial positions of the stiffener.

Fig.(11) and Fig.(12) show the variation in maximum Von-Mises stresses and maximum deflections

respectively, with the ring position (r) for these cases.

Thickness of the diaphragm used is (h= 0.1mm.) and dimensions of the rings are (H= 0.1mm. , br = 2mm.).

➢ **Optimum Position :** To show the optimum ring position, which gives minimum Von-Mises stress and maximum deflection, Fig.(13) is drawn; were, (S_1) represents the maximum Von-Mises stresses of stiffened diaphragm (ring on one surface only) divided by the maximum Von-Mises stress of flat diaphragm, (S_2) represents the maximum Von-Mises stresses of stiffened diaphragm (ring on two surfaces) divided by the maximum Von-Mises stress of flat diaphragm, (S) represents the maximum Von-Mises stress of stiffened diaphragm (clamped ring) divided by the maximum Von-Mises stress of flat diaphragm, and (D) represents the maximum deflections of stiffened diaphragm (ring on one or two surfaces) divided by the maximum deflection of flat diaphragm.

From these non-dimensional curves, the optimum position appears at (r = 35mm.) for using a ring on one or two surfaces.

➢ **Optimum Case of Using Two Rings :** *Mohammed M. Hasan* [14] found that the best choice of using two ring-shaped concentric ribs is the use of clamped ring with minimum thickness (H) and a certain radial width (br) and another ring at the optimum position with high thickness and a certain radial width (this would appear clearly from the results of comparison with the published data).

So, three cases of using two rings are presented here :

- ***Case (1)* :** clamped ring on one or two surfaces (H= 0.1mm. , br = 10mm.), and another (at the optimum position) on two surfaces (H= 0.5mm. , br = 2mm.).
- ***Case (2)* :** clamped ring on one or two surfaces (H= 0.1mm. , br = 10mm.), and another (at the optimum position) on two surfaces (H= 0.4mm. , br = 10mm.).
- ***Case (3)* :** clamped ring on one or two surfaces (H= 0.1mm. , br = 10mm.) and another (at the optimum position) on two surfaces (H= 0.5mm. , br = 10mm.).

The results of these cases with the percentage reduction in maximum Von-Mises stress are recorded in table (1).

➢ **Comparison with a Published Research :** As explained previously, a model similar to that of the published research [1] is built in *MSC/NASTRAN* program under the same conditions.

The author of this published research did not mention anything about his choice to the dimensions and positions of the two rings he used; the only thing he had explained is that the diaphragm was strengthened by these two ring-shaped concentric ribs.

As shown in Fig.(10), the two rings used in [1] were of the same dimensions (H= 6mm., br = 4mm.) at radial positions (r_1 = 20mm., r_2 = 60mm.).

So, eleven different cases are used here to choose the optimum positions and dimensions of the stiffeners, and to compare the published data. These cases are :

- ***Case (1)* :** one ring (clamped ring) on one or two surfaces (H= 6mm. , br = 4mm.).

- ***Case (2)*** **:** one ring (clamped ring) on one or two surfaces (H= 0.6mm. , br = 4mm.).
- ***Case (3)*** **:** one ring (clamped ring) on one or two surfaces (H= 0.6mm. , br = 10mm.).
- ***Case (4)*** **:** one ring (at the optimum position) on one or two surfaces (H= 6mm. , br = 4mm.).
- ***Case (5)*** **:** one ring (at the optimum position) on one or two surfaces (H= 10.5mm. , br = 4mm.).
- ***Case (6)*** **:** one ring (at the position which gives minimum stress) on one surface (H= 6mm., br = 4mm.).
- ***Case (7)*** **:** one ring (at the position which gives minimum stress) on two surfaces (H= 6mm., br = 4mm.).
- ***Case (8)*** **:** two rings [both case (1) and case (4)].
- ***Case (9)*** **:** two rings [both case (1) and case (6)].
- ***Case (10)*** **:** two rings [both case (1) and case (7)].
- ***Case (11) { the optimum choice }*** **:** two rings [both ***case (3)*** and ***case (5)***].

The results of maximum Von-Mises stresses, maximum deflections and the percentage reduction in maximum Von-Mises stress of the above cases are shown in table (2).

5.Dynamic Analysis

This part presents the analysis of stresses and deflections of clamped circular diaphragm subjected to dynamic pressure. All of the models used here are of the same dimensions and properties of those used in static part, and subjected to uniform dynamic pressure with two types of transient loading as discussed previously. Fig.(14) shows the continuous positive sine function (f = 40 Hz., $P_{max.}$= 250 Pa), which is used for all models, and Fig.(15) shows the pulse function with (f = 72.3Hz., $P_{max.}$= 250 Pa), which is used for the flat diaphragm of the base model.

➢ **Effect of Radial Position of The Ring :** To show the effect of using ring-shaped ribs on the two surfaces of the diaphragm instead of one surface, and the effective use of clamped ring, one hundred cases are used here at twenty five radial positions of the stiffener.

Fig.(16) and Fig.(17) show the variation in maximum Von-Mises stresses and maximum deflections respectively, with the radial position of the ring (r), for continuous loading (f = 40 Hz., $P_{max.}$ = 250 Pa).

On the other hand, Fig.(18) and Fig.(19) show the variation in maximum Von-Mises stresses and maximum deflections respectively, with the radial position of the ring (r), for sine-pulse loading [$f = f_n$ (mode 1), $P_{max.}$ = 250 Pa].

Thickness of the diaphragm used is (h= 0.1mm.) and dimensions of the rings are (H= 0.1mm. , br = 2mm.).

➢ **Optimum Position :** To show the optimum ring position (which gives minimum Von-Mises stress and maximum deflection), Fig.(20) and Fig.(21) are drawn for continuous and pulse loading respectively; were, (S_1) represents the maximum Von-Mises stresses of stiffened diaphragm (ring on one surface only) divided by the maximum Von-Mises stress of flat diaphragm, (S_2) represents the maximum Von-Mises stresses of stiffened diaphragm (ring on two surfaces) divided by the maximum Von-Mises stress of flat diaphragm, (S) represents the maximum Von-Mises stress of stiffened diaphragm (clamped ring) divided by the maximum Von-Mises stress of flat diaphragm, and (D)

represents the maximum deflections of stiffened diaphragm (ring on one or two surfaces) divided by the maximum deflection of flat diaphragm.

From these non-dimensional curves, the optimum position appears at (r = 35mm.) for both continuous and sine-pulse loading (ring on one or two surfaces).

6.Conclusions : Clamped circular diaphragms may be strengthened by one or more ring-shaped rib in order to reduce the stresses, when a static or dynamic pressure is applied. However, the proper choice to the dimensions and positions of stiffeners may give optimum results; otherwise, random use of these stiffeners may give opposite results. To get minimum stresses and maximum deflections, a ring-shaped rib with a certain dimensions may be used on one or two of the diaphragm surfaces, at a radial position equal to (70%) of diaphragm radius. On the other hand, a ring-shaped rib can be divided into two equal layers to be used on both of the two diaphragm surfaces instead of one, to get better results for a certain choices. The optimum choice for using two ring-shaped concentric ribs is that of using a clamped ring with the favorite thickness and a certain radial width, and another ring with certain dimensions at the optimum position.

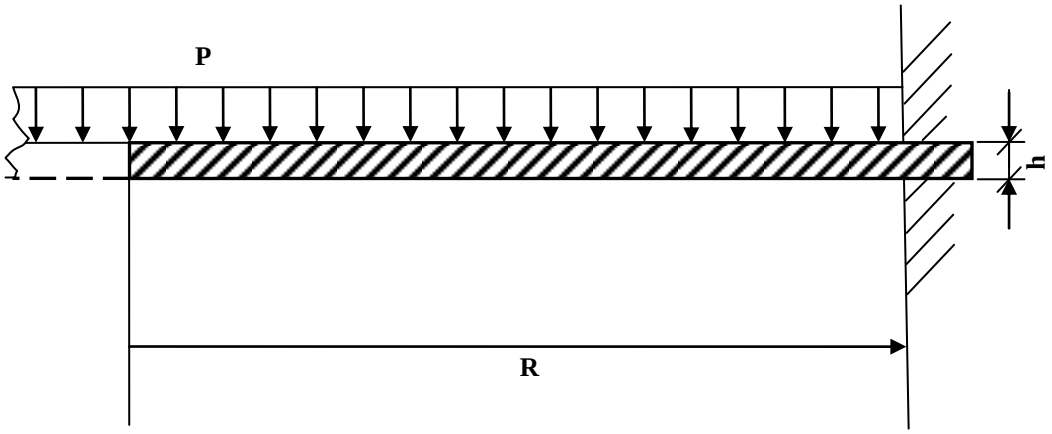

Fig.(1) The schematic view of the base model
(flat diaphragm).

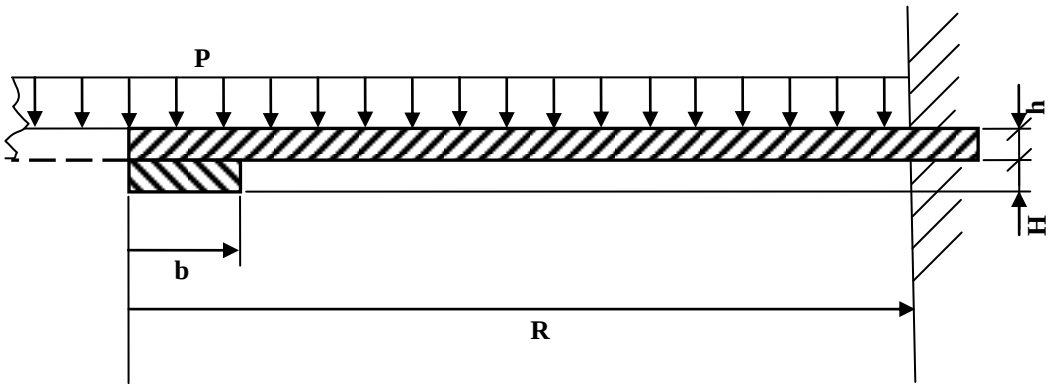

Fig.(2) The schematic view of the bossed diaphragm
(one surface).

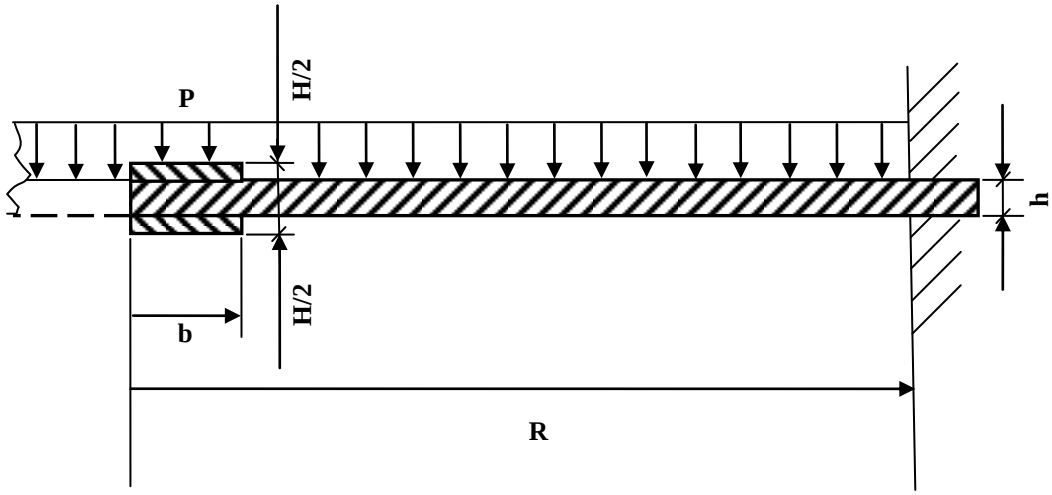

Fig.(3) The schematic view of the bossed diaphragm
(two surfaces).

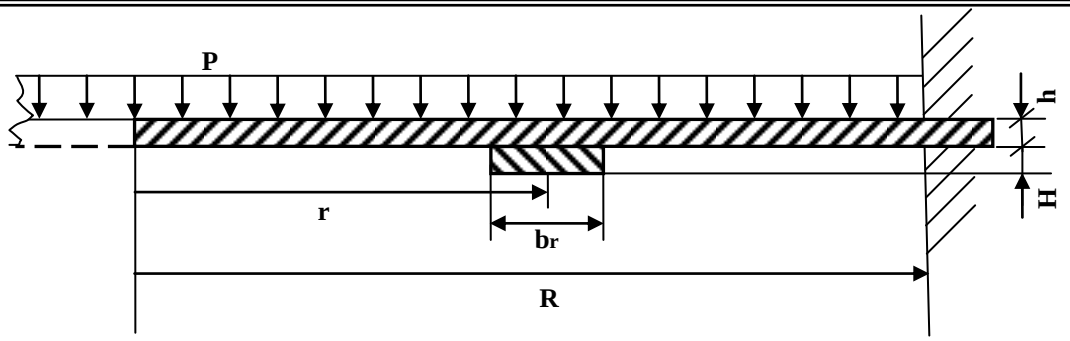

Fig.(4) The schematic view of the stiffened diaphragm (one ring on one surface).

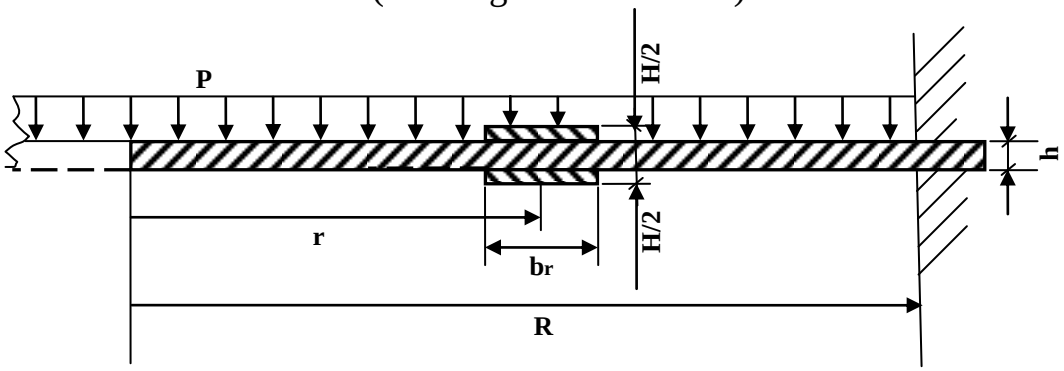

Fig.(5) The schematic view of the stiffened diaphragm (one ring on two surfaces).

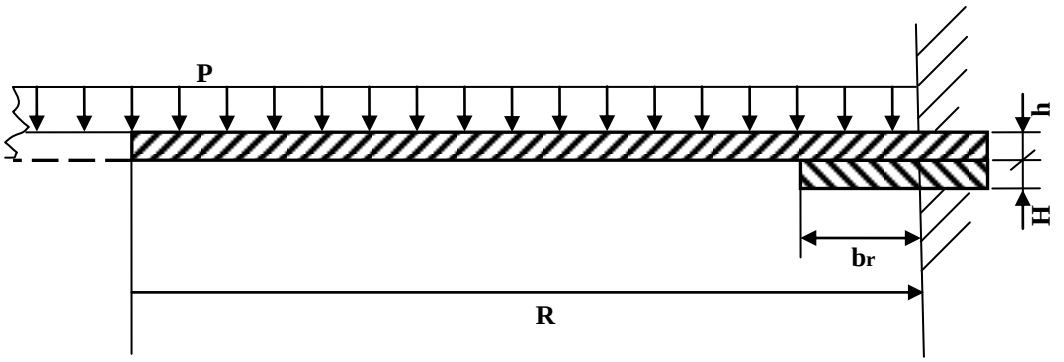

Fig.(6) The schematic view of the stiffened diaphragm (clamped ring on one surface).

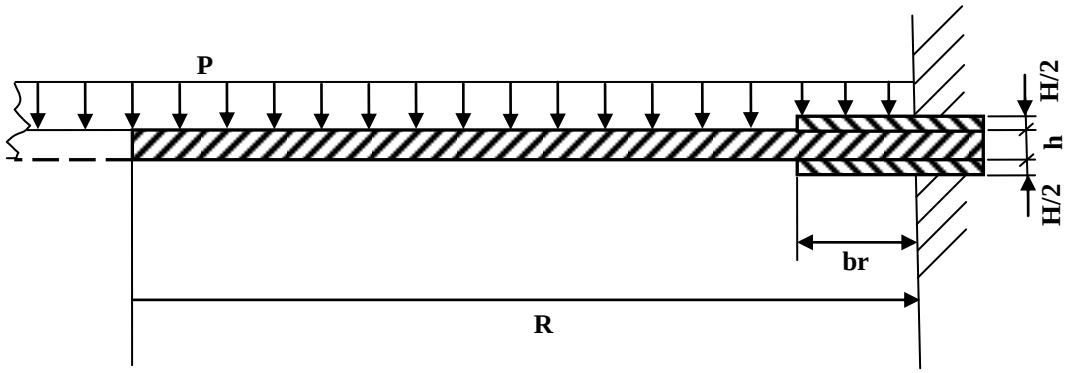

Fig.(7) The schematic view of the stiffened diaphragm (clamped ring on two surfaces).

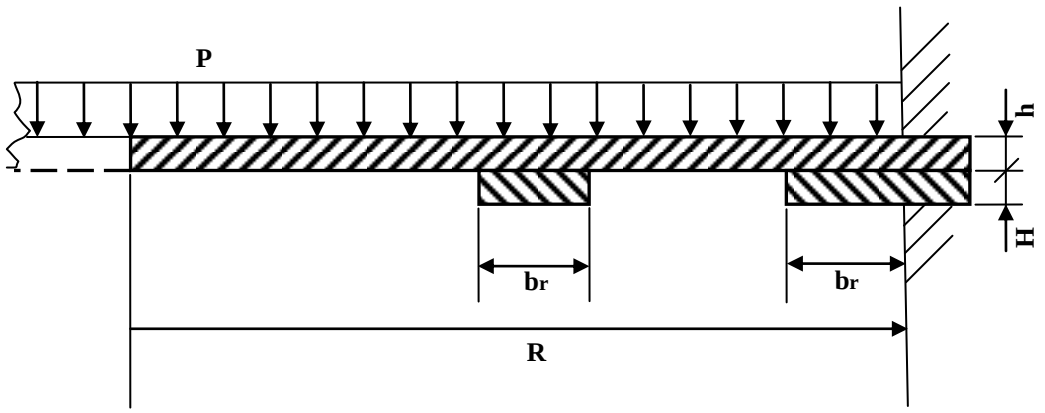

Fig.(8) The schematic view of the stiffened diaphragm
(two rings on one surface).

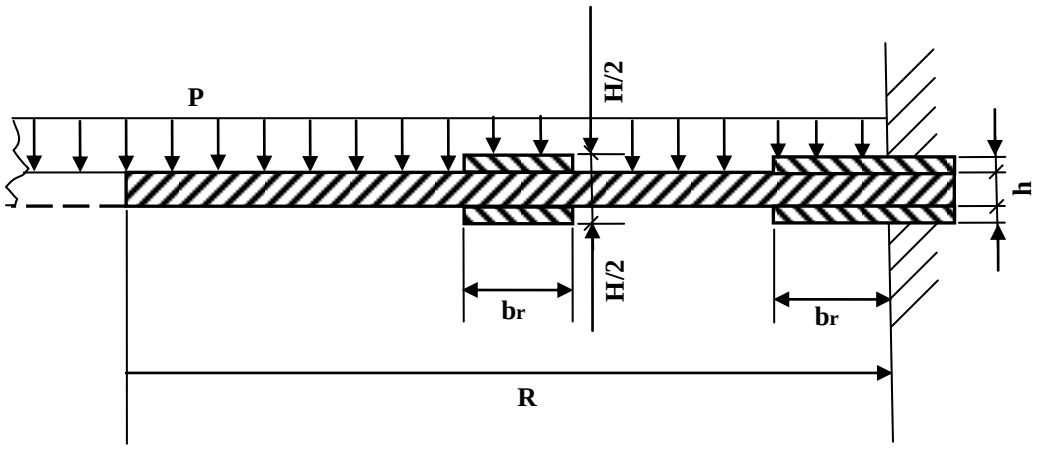

Fig.(9) The schematic view of the stiffened diaphragm
(two rings on two surfaces).

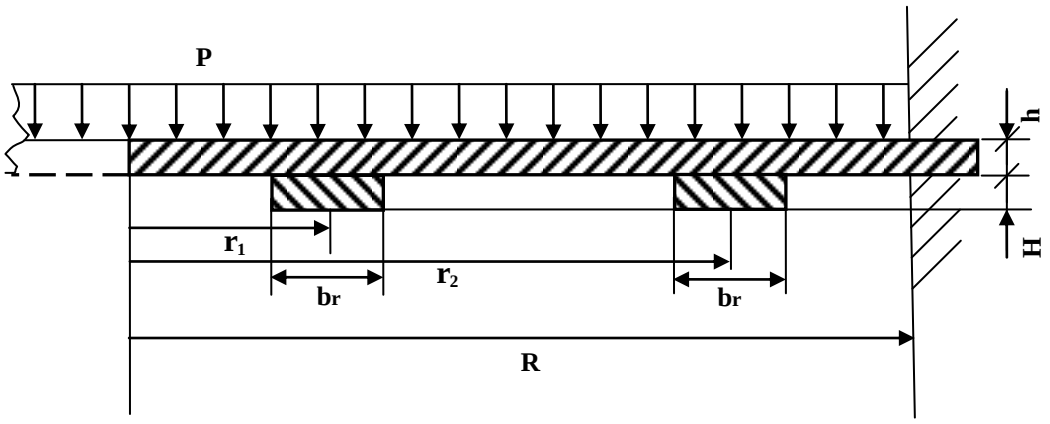

Fig.(10) The schematic view of the model, which had been used in the published research [1].

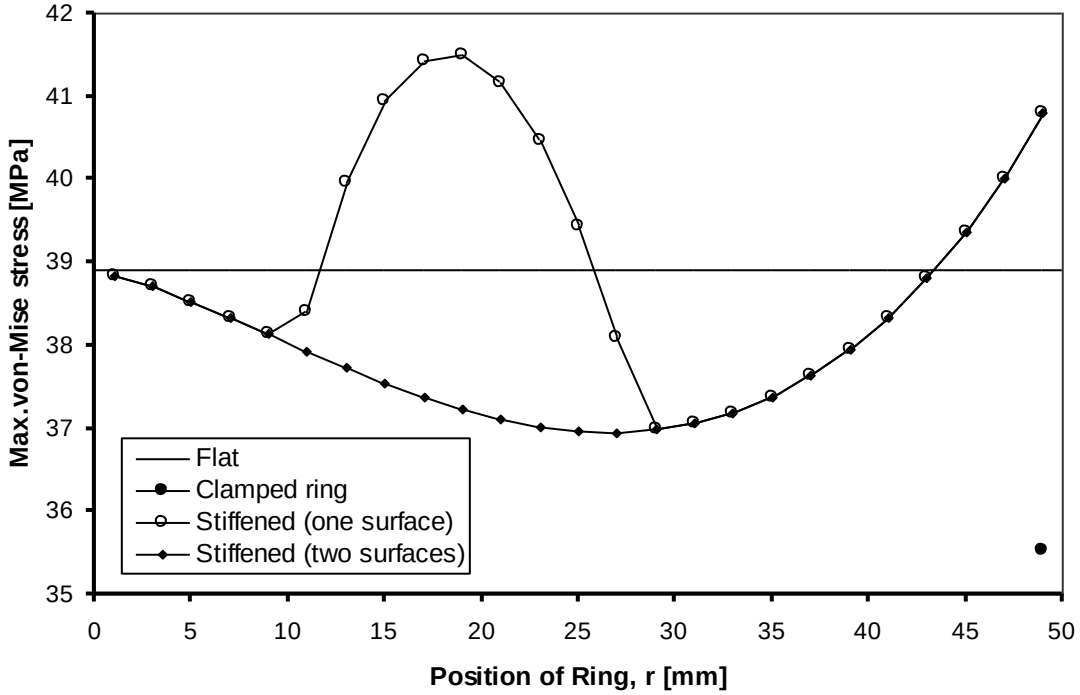

Fig.(11) Effect of radial position of the ring on the maximum Von-Mises stress.

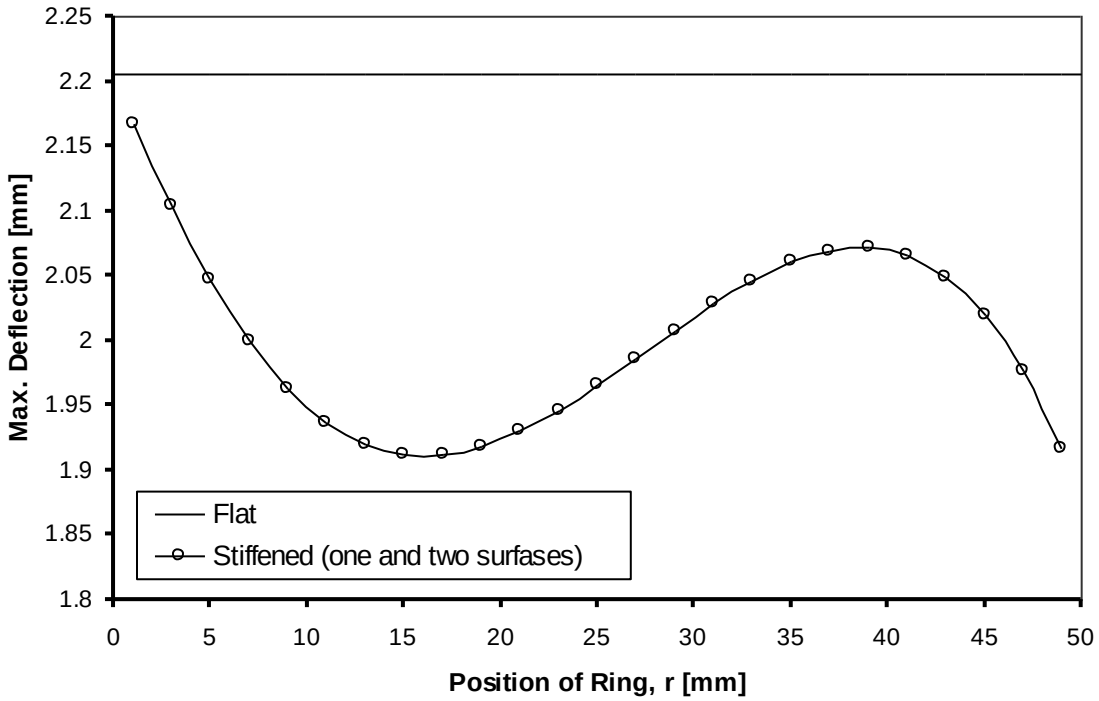

Fig.(12) Effect of radial position of the ring on the maximum deflection.

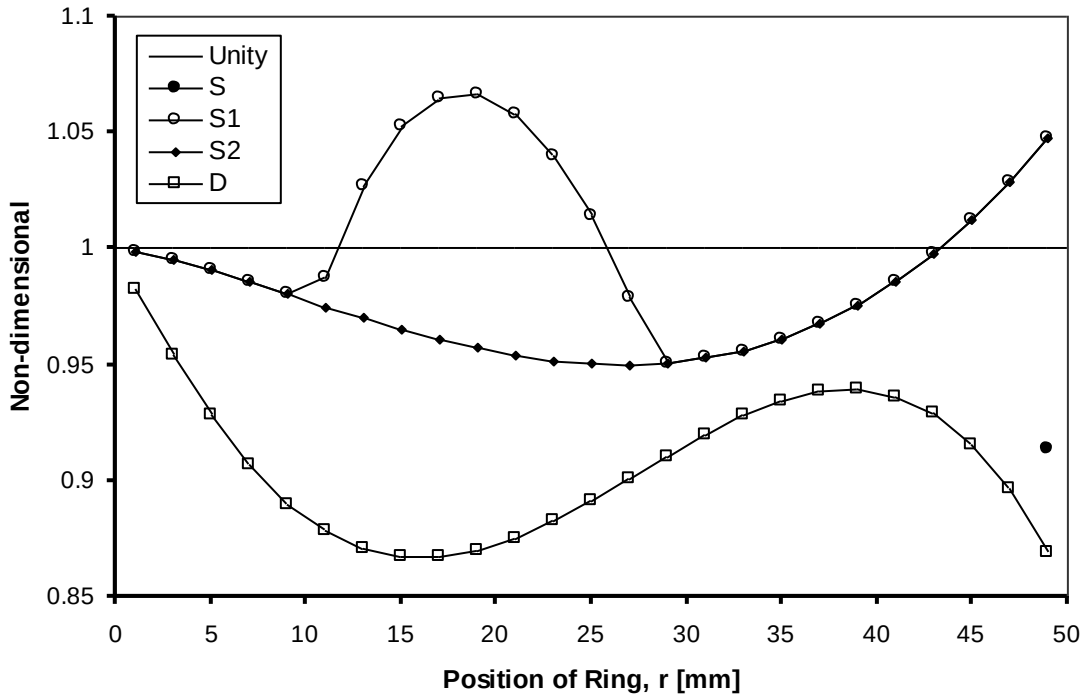

Fig.(13) Non-dimensional representation of stresses and deflections.

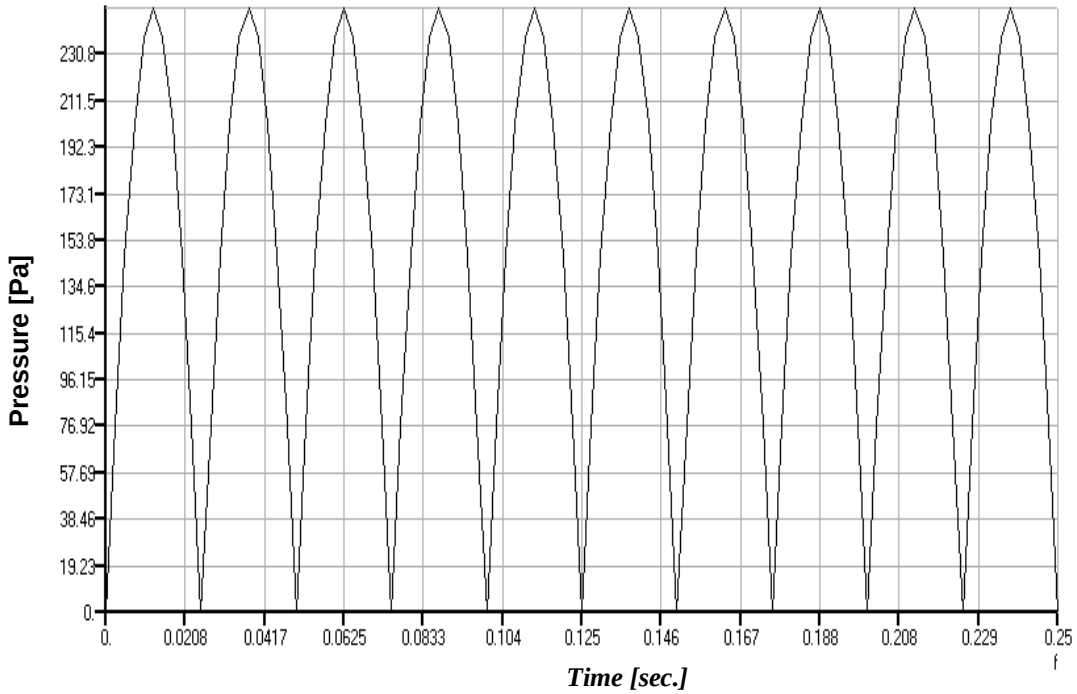

Fig.(14) Continuous sine-function used for all models
(f = 40 Hz., P_{max} = 250 Pa).

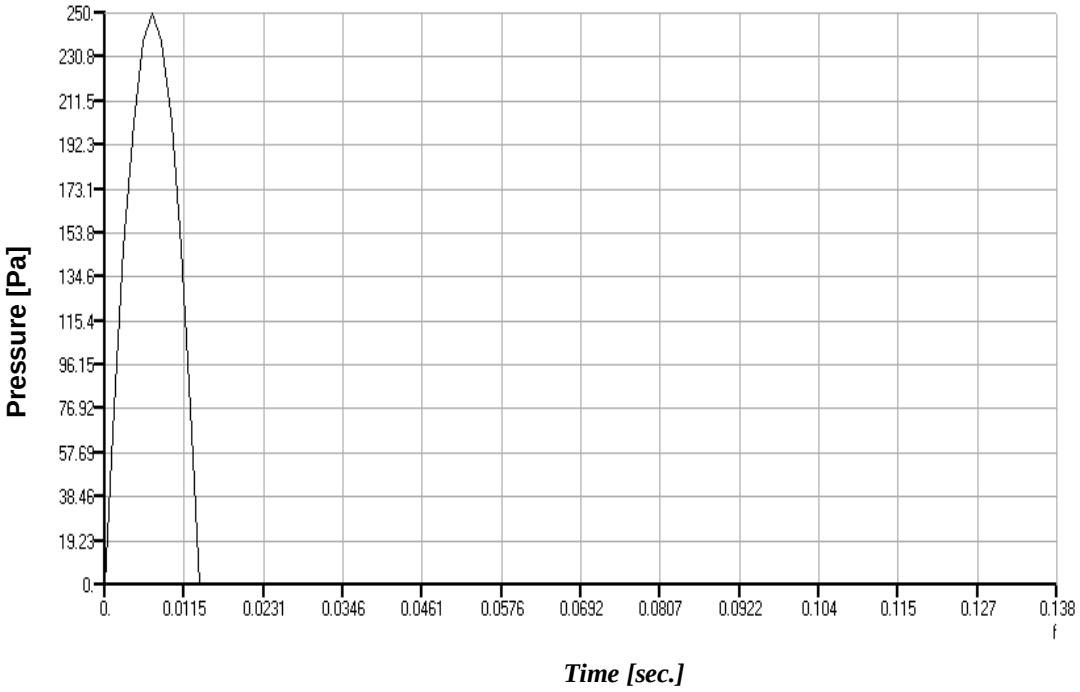

Fig.(15) Sin-pulse function used for flat diaphragm (f = 72.3 Hz., P_{max} = 250 Pa).

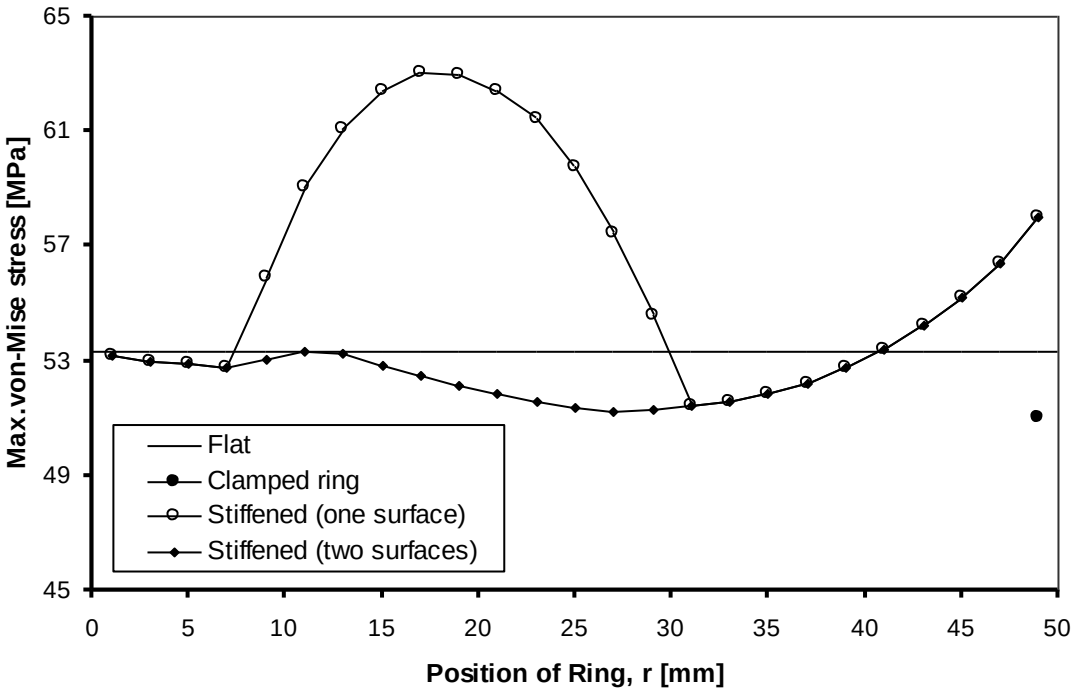

Fig.(16) Effect of radial position of the ring on the maximum Von-Mises stress (continuous loading).

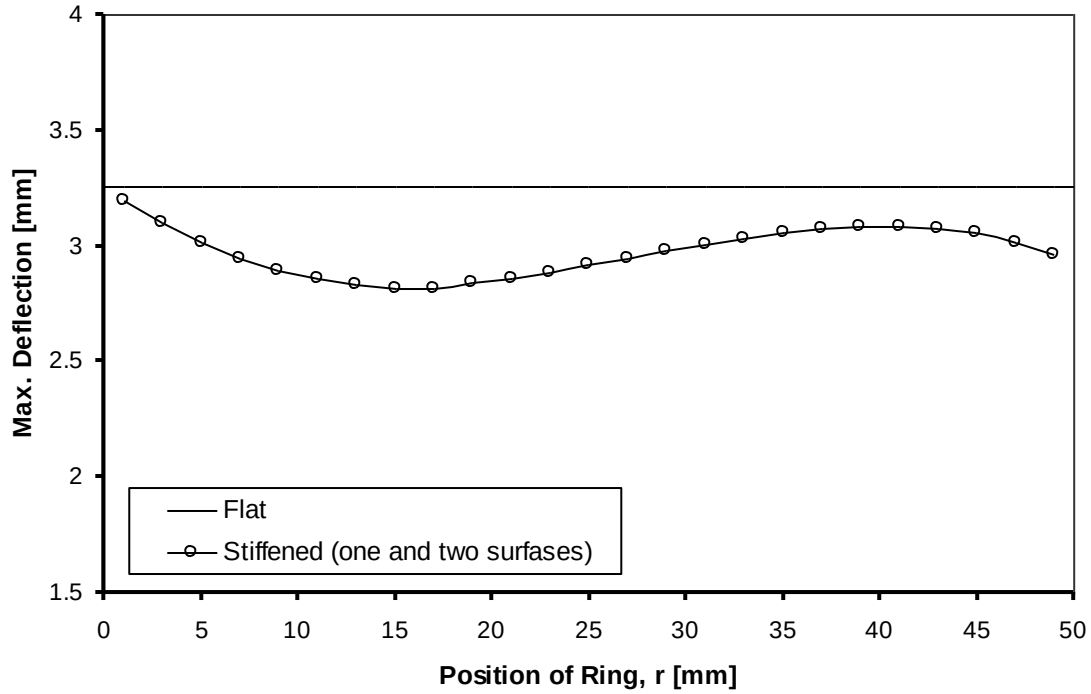

Fig.(17) Effect of radial position of the ring on the maximum deflection (continuous loading).

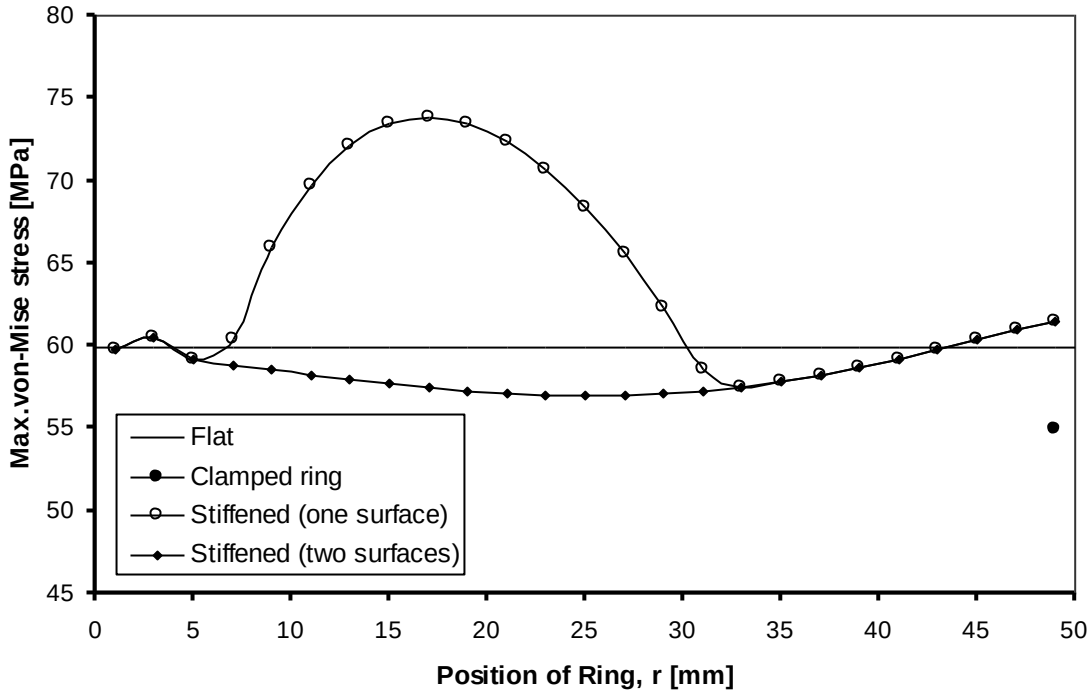

Fig.(18) Effect of radial position of the ring on the maximum Von-Mises stress (sine-pulse loading).

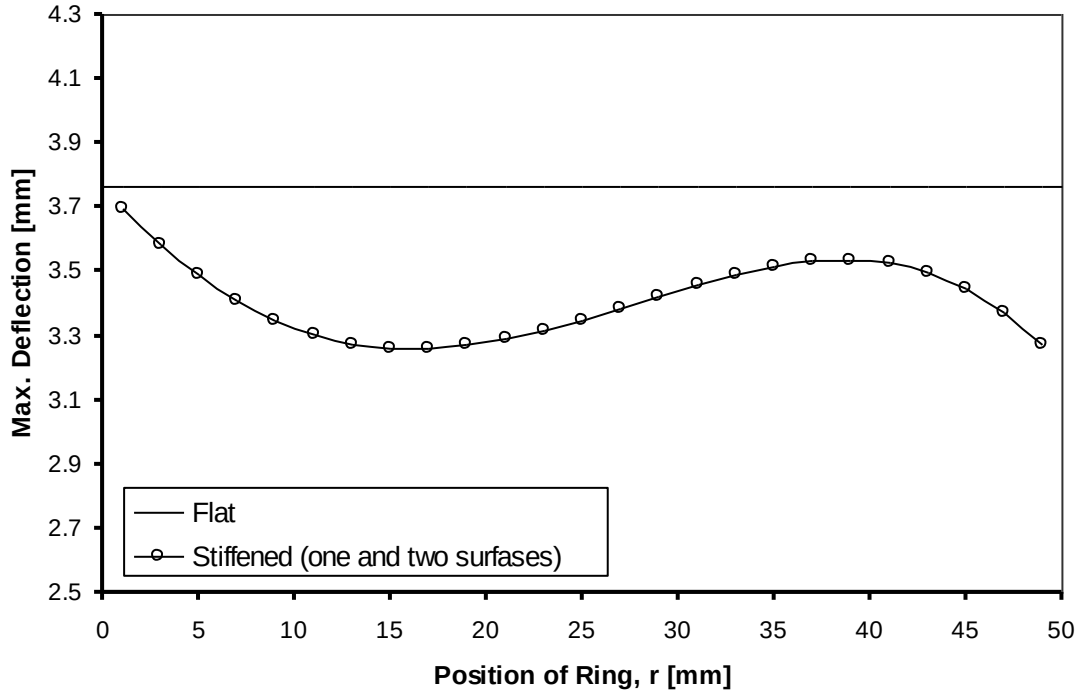

Fig.(19) Effect of radial position of the ring on the maximum deflection (sine-pulse loading).

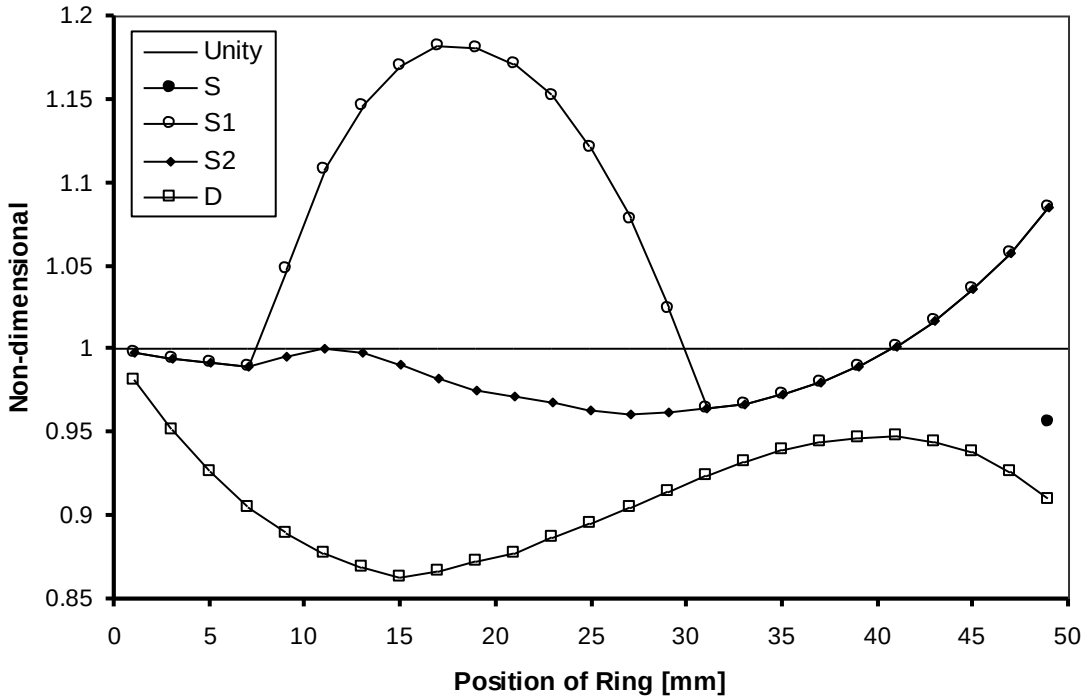

Fig.(20) Non-dimensional representation of stresses and deflections (continuous loading).

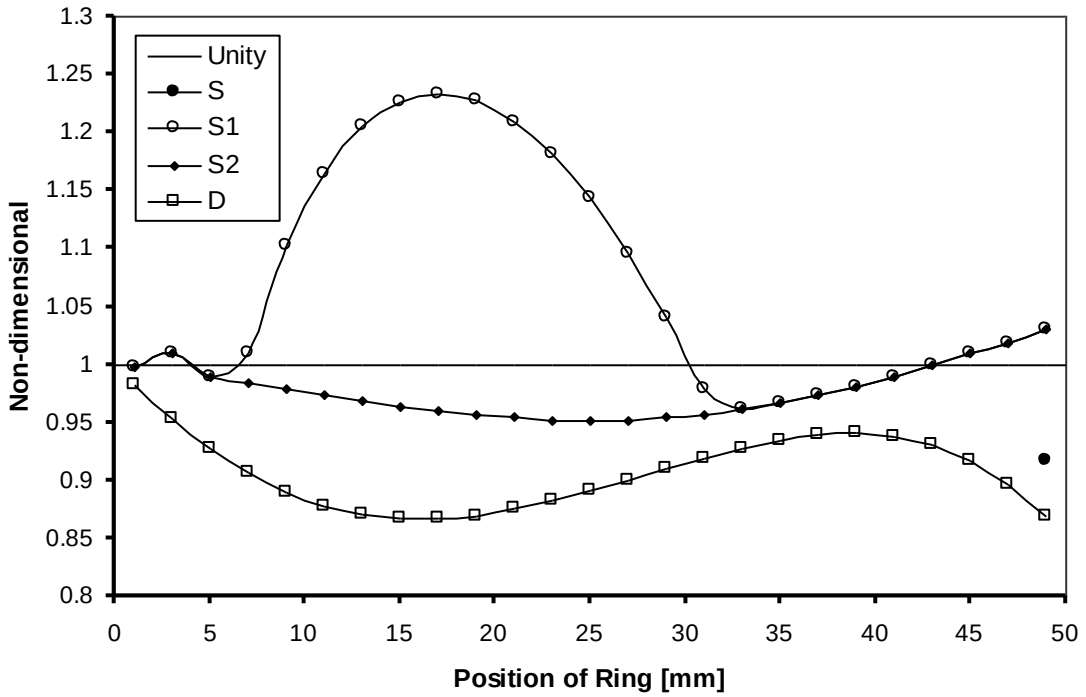

Fig.(21) Non-dimensional representation of stresses and deflections (sine-pulse loading).

Cases	Max. Von-Mises Stress [MPa]	Max. Deflection [mm.]	Percentage Reduction in Max. Von-Mises stress
Flat	38.9	2.206	-----
Case (1)	17.183	0.734	55.83 %
Case (2)	12.83	0.442	67.02 %
Case (3)	12.65	0.401	67.5 %

Table (1)
Stiffened diaphragm (two rings).

Cases	Max. Von-Mises Stress [KPa]	Max. Deflection [mm.]	Percentage Reduction in Max. Von-Mises stress
Flat	669.6	12.186	-----
Ref.[1]	604.5	8.5	9.72 %
Case (1)	595.7	9.977	11.04 %
Case (2)	566	11.417	15.47 %
Case (3)	542.3	10.619	19 %
Case (4)	623.2	10.823	6.93 %
Case (5)	538.87	9.274	19.52 %
Case (6)	606.28	10.28	9.46 %
Case (7)	605.14	9.773	9.63 %
Case (8)	551.77	8.882	17.6 %
Case (9)	538.48	8.51	19.6 %
Case (10)	534.4	8.06	20.2 %
Case (11)	462.2	8.4	31 %

Table (2)
Comparison between present work and the published [1].

Nomenclature		
Symbol	***Description***	***Unit***
br	Redial width of the ring	m.
E	Modulus of elasticity	N/m^2(Pa)
f	Frequency	Hz.
G	Modulus of rigidity	N/m^2(Pa)
h	Diaphragm thickness	m.
H	Ring thickness	m.
P	Pressure	N/m^2(Pa)
P_y	Yield pressure	N/m^2(Pa)
r	Redial position of the stiffener	m.
R	Diaphragm radius	m.
t	time	sec.
ν	Poisson's ratio	---
ρ	Mass density	Kg/m^3
σ_y	Yield stress	N/m^2(Pa)
ω	Circular frequency	rad./sec.

7.References

[1] Zlatan Kulenović, ***Analytical and Experimental Analysis of Stresses and Deflections of Strengthened Diaphragm***, International Design Conference – Design 2000, Dubrovnik, May 23 – 26, 2000.
[Online] Available http://www.io.tudelft.nl/research/ica/index_publication.html

[2] ***Procedures for Diaphragms.***
[Online] Available http://www.oshpd.cahwnet.gov/fdd/About_Us

[3] R. Steinmann, H. Friemann, C. Prescher, and R. Schellin, ***Sensors and Actuators A***, 48, pp. 37-46,1995.
[Online] Available http://www.el.utwente.nl/tt/publications

[4] D. Maier-Schneider, J. Maibach, and E. Obermeier, ***Journal of Microelectromechanical Systems***, 4(4), pp. 238-241,1995.
[Online] Available http://touch.caltech.edu/publications/shuyun/mems95

[5] E.H. Yang, S.W. Han and S.S. Yang, ***Fabrication and testing of a pair of passive bivalvular microvalves composed of p + silicon diaphragms***, Sensors and Actuators A 57, pp.(75-78), 1996.
[Online] Available http://www.elsevier.nl/locate/sna

[6] Rahul Saini, Sunil Bhardwaj, Toshikazu Nishida and Mark Sheplak, ***Scaling Relations for Piezoresistive Microphones***, Proceedings of IMECE, International Mechanical Engineering Congress and Exposition, November 5-10, 2000, Orlando, Florida.
[Online] Available http://www.me.bringhamton.edu/miles

[7] W.P. Eaton, Fernando Bitsie, J.H. Smith, and David W. Plummer, ***A New Analytical Solution for Diaphragm Deflection and its Application to a Surface-Micromachined Pressure Sensor***, Technical Proceedings of the International Conference on Molding and Simulation of Microsystems,1999.
[Online] Available http://www.comppub.com/publication/MSM/99/pdf

[8] Klaus-Jürgen Bathe, ***Finite Element Procedures***, Prentice-Hall International, Inc., 1996.

[9] Tirupathi R. Chandrupatla and Ashok D. Belegundu, ***Introduction to Finite Elements in Engineering***, Prentice-Hall of India, Private Limited, New Delhi, 1996.

[10] ***Copper.***
[Online] Available http://www.hyperphysics.phy-astr.gsu.edu

[11] ***Mechanical Properties of Materials***, Spring 2002.
[Online] Available http://web.mit.edu/3.22/www/ps8.pdf

[12] Joseph Edward Shigley, ***Mechanical Engineering Design***, First Metric Edition, McGraw-Hill book company, 1986.

[13] E.J. Hearn, ***Mechanics of Materials***, second Edition, Pergman Press Ltd., 1985.

[14] S.P. Timoshinko and K.S. Woinowsky, Theory of Plates and Shells, Second Edition, Tokyo, McGraw-Hill Kogakusha Ltd, 1959.

[15] Mohammed M. Hasan, ***Theoretical and Experimental Investigation of Stresses and Deflections of Stiffened Diaphragm Subjected to Dynamic Pressure,*** M.Sc. Thesis, University of Al-Anbar, College of Engineering, Department of Mechanical Engineering, 2002.

د.سومر متي ناسي قسم هندسة عمليات التصنيع كلية هندسة الخوارزمي جامعة بغداد

د.حكمت الراوي جامعة الانبار

محمد م.حسن جامعة الانبار

الخلاصة:

تناول هذا البحث دراسة الاجهادات و الانحرافات في الأغشية الدائرية والمقواة بحلقة أو حلقتين مركزيتين تحت تأثير ضغط استاتيكي أو ديناميكي منتظم . تمت عملية النمذجة باستخدام طريقة العناصر المحددة من خلال برامجية Nastran .

لإجراء دراسة تصميمية جديدة تم الأخذ بنظر الاعتبار تأثير حلقة التقوية المثبتة في الجوانب وتأثير تثبيت حلقات التقوية على سطحي الغشاء . لبيان فعالية نتائج هذه الدراسة تمت المقارنة مع نتائج المصدر (1) .

من نتائج هذه الدراسة يمكن استخلاص صلاحية التصميم الامثل للأغشية المقواة .